Published in final edited form as:
ACS Nano. 2017 November 28; 11(11): 11264–11272. doi:10.1021/acsnano.7b05631.

Directional Photonic Wire Mediated by Homo-Förster Resonance Energy Transfer on a DNA Origami Platform

Francesca Nicoli[#1], **Anders Barth**[#2], **Wooli Bae**[1], **Fabian Neukirchinger**[1], **Alvaro H. Crevenna**[2,3], **Don C. Lamb**[2,‡], and **Tim Liedl**[1,‡]

[1]Department of Physics and Center for Nanoscience, Ludwig Maximilians University, Munich, Germany

[2]Department of Chemistry and Biochemistry and Center for Nanoscience, Ludwig Maximilians University, Munich, Germany

[#] These authors contributed equally to this work.

Abstract

Elaborating new strategies and deepening the understanding of light transport at the nanoscale is of great importance for future designs of artificial light harvesting assemblies and dye-based photonic circuits. In this work, we focus on studying the phenomenon of Förster resonance energy transfer (FRET) amongst fluorophores of the same kind (homo-FRET) and its implications for energy cascades containing two or three different dye molecules. Utilizing the spatial programmability of DNA origami, we arranged a chain of Cyanine 3 (Cy3) dyes flanked on one end with a dye of lower excitation energy Cyanine 5 (Cy5) without or with an additional dye of higher excitation energy, Alexa488, on the other end. We characterized the response of our fluorophore assemblies with bulk and single-molecule spectroscopy and support our measurements by Monte Carlo modelling of energy transfer within the system. We find that, depending on the arrangement of the fluorophores, homo-FRET between the Cy3 dyes can lead to an overall enhanced energy transfer to the acceptor fluorophore. Furthermore, we systematically analyzed the homo-FRET system by addressing the fluorescence lifetime and anisotropy. Finally, we built a homo-FRET-mediated photonic wire capable of transferring energy through the homo-FRET system from the blue donor dye (Alexa488) to the red acceptor fluorophore (Cy5) across a total distance of 16 nm.

[‡]Correspondence to tim.liedl@physik.lmu.de and d.lamb@lmu.de.
[3]Current address: Instituto de Tecnologia Química e Biológica António Xavier, Universidade Nova de Lisboa, 2780-157 Oeiras, Portugal

Author contribution

F.N. and T.L. designed the study and planned experiments. F.N. and F. Neu. fabricated the samples, performed and analyzed the ensemble measurements. A.B. and D.L. planned the single molecule experiments. A.B. performed and analyzed the single molecule experiments. F.N., W.B. and T.L. planned the Monte Carlo simulation and W.B. performed the simulations. All authors have read and contributed to the manuscript.

The authors declare no competing financial interest.

Europe PMC Funders Author Manuscripts

Keywords

Artificial light harvesting; homo-FRET; DNA origami; photonic wires; energy transfer; single molecule FRET

Introduction

The phenomenon of light migration via resonant energy transfer is of fundamental importance in nature. In photosynthetic organisms,1–3 light is absorbed by pigments located in the light harvesting complexes (LHCs) and then transferred through different mechanisms to the reaction center, where the photons are transformed into chemical energy.1,4,5 Energy transfer on the sub-nanometer length scale between the pigment molecules within the LHC occurs mainly through coupled excitons. Over longer distances (> 1 nm), the energy is transferred through dipole-dipole interactions by means of resonance energy transfer.5,6,7 To understand and mimic the natural process of light harvesting, it is beneficial to construct artificial systems that efficiently control the transport of light. Great success has already been achieved in creating complex arrangements of dyes and LHCs on different biological platforms such as lipid membranes8–11 and protein capsids.12,13 The ability of collecting light with dye clusters is also utilized in dye-sensitized solar cells.14 Here, inspired by the basic principle of nature's light harvesting mechanisms, we designed a DNA origami nanostructure to investigate long-range energy transfer by creating a linear arrangement of three spectrally different dyes. The resulting energy landscape allows the light to be transferred from the excited donor dye through a number of identical transmitter dyes to a single acceptor fluorophore. We investigate the contributions of the different fluorophores to the energy cascade coming from hetero-FRET (energy transfer between two different fluorophores) and homo-FRET (energy transfer between fluorophores of the same kind). Since DNA can be used as a rigid and easily modifiable scaffold for positioning molecules at precise distances and in many different configurations,15–17 extensive work has been done on constructing photonic networks for light harvesting and photonic circuits on simpler DNA constructs15,18–26 as well as more complex DNA origami nanostructures.16,17,27,28 Previous bulk studies focused on homo-FRET mediated photonic wires, where the energy is transferred from a high-energy donor to a lower energy acceptor through a chain of equal energy dyes. Performing FRET studies on DNA origami provides some advantages over simpler double-stranded DNA structure.18,19,21–23 DNA origami offers an efficient and robust way to arrange a large number of dyes in different configurations. In fact, by simply exchanging a few specific oligonucleotides, the same structure can be utilized to place different species of dye molecules or other nanocomponents27,29,30 with nanometer precision in almost arbitrary arrangements in a single plane. Furthermore, the components can be assembled with finely controlled stoichiometry while DNA structures consisting of few strands often require tedious tailoring of DNA strand ratios to achieve a good assembly quality. Another important aspect of using DNA origami for reliable optical characterization is the effectiveness of the purification steps, where it is straightforward to separate large DNA origami objects from individual oligonucleotides or dye molecules.

Europe PMC Funders Author Manuscripts

Here, we assembled a combination of a three-color cascade and a homo-FRET-based photonic wire (PW), achieving energy transfer over a distance of 16 nm from a blue donor dye to a red acceptor dye through three green fluorophores. We focus on the effects of homo-FRET on the overall energy transfer. Specifically, we break down the complex dye cascade into its individual components and, through a systematic analysis of the partial contributions of each dye to the system, we show that the overall energy migration is enhanced by homo-FRET between the donors, as compared to expected transfer efficiency in the absence of homo-FRET. We carried out bulk fluorescence spectroscopy measurements as well as single-molecule (SM) experiments measuring the FRET efficiency, fluorescence lifetime and fluorescence anisotropy. Finally, Monte Carlo (MC) simulations were performed to obtain a consistent picture of the energy transfer processes.

Results and Discussion

A schematic drawing of the DNA-origami supported PW is shown in Figure 1 A. The full PW consists of five dyes: one blue donor (Alexa488) with the highest excitation and emission energies, three green dyes (Cy3) of intermediate energies and one acceptor (Cy5) exhibiting the lowest energies. The dyes are positioned in a quasi-linear arrangement on the upper surface of a three-layered DNA origami block, resembling a 1D-wire. The different labeling positions for Cy3 are indicated with a "G_1", "G_2" or "G_3" when the respective dye is present, while an "X" indicates the absence of any dye in that position (Figure 1B and SI 1 Table S1 for the complete list of all constructs). As the blue and red fluorophore are separated by 16 ± 0.6 nm (the distances and corresponding errors are based on the well-known structure of DNA origami objects and the flexibility of the linker molecule), energy absorbed from the blue donor to the red acceptor must travel through a multi-step energy transfer process *via* one or more intermediate green dyes. Of the multiple possible energy pathways, the most important ones are shown in Figure 1 C. The spectral characteristics of the dyes are illustrated in Figure S1 and discussed in SI 2.

For the homo-FRET system, we determined a Förster radius of 4.6 nm, resulting in expected transfer efficiencies in an isolated system of 90% (G_2G_3), 50% (G_1G_2) and 27% (G_1G_3) between Cy3s in our PW. We assume the dipole-dipole interaction regime, as the minimum separation between the fluorophores is larger than 3 nm.

We first investigate the system with a single acceptor dye and no blue dye, a condition inspired by the energy migration in the LHC from multiple donors to a single acceptor acting as an energy sink, meaning that by accepting energy the chromophore actively depletes the system. To determine the overall energy transfer in this system, we measured bulk fluorescence emission spectra after excitation of the Cy3 fluorophores. Figure 2 shows the spectrum of the construct $G_1G_2G_3R$ with the three homo-FRET green dyes and the red acceptor and the corresponding assembly without acceptor. Clearly the former spectrum exhibit two emission peaks, one from Cy3 around 560 nm and the second one from Cy5 around 660 nm, indicating the occurrence of FRET, while for the latter construct no red emission is detected. To assess the amount of the direct excitation of Cy5 upon 520 nm incident light, we performed a control where we mixed in a 3 to 1 ratio the fluorescently labeled DNA staples corresponding to the three green and the one red staple and measured

the emission spectrum. A negligible amount of red fluorescence is detected (see inset in Figure 2 and Figure S2 and SI 3 for the quantification of Cy5 absorption at 520 nm).

To investigate the effect of homo-FRET on the energy transfer, we measured the emission from the single Cy3/Cy5 hetero-FRET pairs (G_1XXR, XG_2XR and XXG_3R) and compared $G_1G_2G_3R$. This assembly shows a significant increase in Cy5 fluorescence compared to the constructs with only one donor. The measured increase in absolute fluorescence is expected in hetero-FRET systems from the contribution of multiple donors.17 To quantify the contribution of multiple donor dyes on the energy transfer, we compared the sum of the individual Cy3/Cy5 pairs to the full construct (Figure 3 A grey spectrum). Overall, we found that this energy delocalization results in a small increase of Cy5 emission compared to the sum of the single contributions of G_1, G_2 and G_3. When calculating the corresponding energy transfer efficiency, we find that the three donor construct leads to an increase of $\Delta E = 0.01$, compared to the averaged contribution of single hetero-FRET pairs. This increase corresponds to an enhancement of 7.5% (see Table 1 and SI 3 and SI 4 for bulk efficiency and enhancement calculations). Due to heterogeneity of samples this increase falls within variability, but it is consistently present in every sample batch measured. It should be noted that, while $G_1G_2G_3R$ has an overall lower FRET efficiency than XXG_3R due to the increasingly larger distance between the additional donors G_1 and G_2 from the acceptor, the overall transfer to the acceptor is enhanced as is evident from the increased Cy5 emission.

To analyze all the possible energy transfer pathways, we assembled a series of partial constructs with two green dyes (Figure 3 B-D). For the G_1G_2XR construct, we observe a slight decrease in red emission, compared to the sum of G_1XXR and XG_2XR, while the difference of green emission falls within the sample variability, indicating a slight reduction of the energy transfer efficiency. No consistent difference in energy transfer is observed for G_1XG_3R when compared to the sum of XXG_3R and G_1XXR. The construct XG_2G_3R, on the other hand, shows an energy transfer increase of $\Delta E = 0.04$ as compared to the average contribution of XXG_3R and XG_2XR. This result indicates an enhancement of the energy transfer of about 18% where both hetero- and homo-FRET occur with the highest efficiency. However, in ensemble experiments, an average value is measured and errors arising from variations in dye-DNA labeling efficiencies and incomplete DNA staples incorporation cannot be easily corrected, limiting our understanding of the system

To address these limitations and to obtain complementary data, we performed single-molecule FRET measurements in solution by burst analysis.32 In burst analysis experiments, single molecules are measured at picomolar concentration as they diffuse through the femtoliter-sized observation volume of a confocal microscope on the timescale of a few milliseconds. Fluorescence bursts coming from a single origami are isolated and analyzed. By using pulsed interleaved excitation,32 we can selectively investigate only those construct that carry both an active donor and an active acceptor dye (see SI 6 and Figure S3). The single-molecule FRET results are thus not biased by the efficiency of acceptor strand incorporation into the origami, the labeling efficiency of the acceptor strand nor by long-lived dark states of the fluorophore. In fact, we find that the fraction of constructs missing an active acceptor fluorophore varies between 7 and 23 %, which affects the ensemble results (see SI Table S3).

We measured single-molecule distributions of the green to red energy transfer efficiency again for samples with one Cy5 acceptor and one, two or three Cy3 donors (Figure 3 E-H). Generally, we observe broad distributions of FRET efficiencies beyond what is expected from photon shot-noise even for constructs with a single Cy3 dye. This heterogeneity could be caused by interactions of the dyes with the DNA, which can affect the quantum yield and thus lead to a distribution of observed transfer efficiencies. We obtain mean apparent energy transfer efficiencies of E = 0.06 for G_1XXR, E = 0.13 for XG_2XR and E = 0.45 for XXG_3R, which roughly correspond to what we measured in ensemble FRET experiments.

As before, we compare the average transfer efficiency of the individual Cy3/Cy5 pairs to the average transfer efficiency of the constructs with two or three Cy3 dyes. For the single molecule FRET efficiency histograms, the average FRET efficiencies are given by the dashed lines in Figures 3 E-H. The increased energy transfer efficiency observed in the bulk measurements for constructs $G_1G_2G_3R$ and XG_2G_3R is seen more clearly by the single-molecule measurements, where, compared to the single-Cy3 constructs, we observe an increase in energy transfer of $\Delta E = 0.11$ and $\Delta E = 0.06$, corresponding to an enhancement of 38% and 28% for XG_2G_3R and $G_1G_2G_3R$ respectively. In the ensemble measurements, no enhancement was observed for G_1XG_3R. However, in the single molecule experiments, we measure an energy transfer increase of 27%. This increase in sensitivity in the single molecule experiments comes from ability to only select DNA origami structures with both photoactive donor and acceptor fluorophores. Thus, single molecule experiments are not influenced by the contributions from the donor only species and are more robust for different sample preparations with varying amount of fluorescent labeling. By correcting the ensemble FRET efficiencies using knowledge of the fraction of Cy3-only molecules determined from burst analysis experiments, we find that the quantitative agreement between ensemble and single-molecule experiments is increased (see Table S5). The construct G_1G_2XR shows no significant change in both single molecule and ensemble FRET experiments.

Since homo-FRET can be interpreted as a diffusive process between molecules without preferential direction,13,19,23 in theory no change in the overall transfer efficiency is expected. Given our experimental conditions, saturation effects do not play a role and only one green dye is excited at any time. If the green fluorophores were acting as independent molecules, the emission of the full construct should be equivalent to the sum of the single components i.e. the ensemble of independent energy pathways should be equal to the sum of the parts. Our observations of enhanced energy transfer in the constructs XG_2G_3R and $G_1G_2G_3R$, however, indicate that the dyes are not acting independently but that homo-FRET is contributing to the increase of energy transfer. Previous studies showed that cyanine dyes linked to DNA exhibit Förster behavior down to a distance of ~ 8 base pairs33 and hetero-dimer formation was only observed at distances of < 6 base pairs.33–35 We thus rule out the eventuality of contact quenching and dye-dye strong interactions and consider the role homo-FRET is playing in the energy transfer process. The short distance between the green dyes promotes an efficient energy exchange among them, while the proximity of G_3 to the acceptor dye, which acts as an energy sink, depletes the energy from the homo-FRET system. Here, the hetero-FRET process creates an energy hole on G_3, which can subsequently accept more energy from G_1 and G_2 and again transfer it to the final acceptor.

This mechanism of efficient migration of energy from G_3 to R could explain the increased energy transfer of these constructs. In the G_1XG_3R assembly, only a small enhancement was observed in the ensemble experiments, but a clear enhancement is evident from the single-molecule results. Here, the homo-FRET distance is larger than in the construct $G_1G_2G_3R$ and XG_2G_3R, resulting in a reduced homo-FRET transfer efficiency. In spite of the reduced delocalization of energy over the homo-FRET system, the results indicate that the depletion by G_3 still results in an enhancement of energy transfer. On the other hand, for G_1G_2XR, the lower efficiency of hetero-FRET diminishes the depletion of the homo-FRET system by the energy sink, resulting in no net enhancement for this construct.

As the contribution of a homo-FRET system to energy transfer is not intuitive, we confirmed the enhancement by modeling our photonic wire with Monte Carlo (MC) simulations. The MC simulations were performed using standard theory of Förster-type energy transfer. To better simulate our system, we incorporate the limited rotational freedom of the fluorophores on the origami platform into the calculation. Often, the dipole moments of fluorophores are assumed to rotate freely so that the orientation factor, κ^2, for the FRET efficiency averages to 2/3. However, the attachment of the fluorophores to the flat surface of our DNA construct limits the accessible volume of the dyes. Additionally, the rotational freedom can be partially hindered by the interaction between the dyes and the DNA.33,36,37 These considerations can be implemented by sampling different angle configurations for each energy transfer step in the system. Here, we modeled all the partial and the full homo-FRET constructs assuming isotropic dipole orientations within a half-sphere for the different dyes and no preferential directionality for the energy transfer in the homo-FRET part of the wire. We used the experimental values of FRET efficiency from fluorescence bulk measurements of single hetero-FRET pairs to establish the simulations parameters. For the rate of homo-FRET, we used the expected efficiency values calculated from overlap integral and distance between the green dyes. From the simulations, we obtained overall transfer efficiencies in very good agreement with our bulk experimental values (see Table 1). Importantly, the FRET efficiencies from the MC calculation of homo-FRET constructs also show an increased energy transfer of 16% for XG_2G_3R and 10% for $G_1G_2G_3R$ and a negligible change for G_1XG_3R and G_1G_2XR ($\Delta E < 0.01$).

To investigate homo-FRET in the absence of hetero-FRET, we need to use anisotropy information as the fluorescence lifetime should not change for an ideal homo-FRET system nor can FRET be calculated via spectral shifts. Fortunately, anisotropy data is available from the single-molecule multiparameter fluorescence detection experiments with pulsed interleaved excitation.32 Anisotropy uses the polarization of the excited and emitted photons to measure the orientation of the molecule. The anisotropy decreases due to molecular rotation as well as via energy transfer. Figure 4 A shows the time-resolved anisotropy decay of the various constructs (for constructs carrying two Cy3 dyes see Figure S4). The emitted photons preferentially have the same polarization as the excitation light at short times, which quickly decays. The “dip-and-rise” behavior with an initial fast decay of the anisotropy and subsequent rise to the residual anisotropy value occurs in the presence of distinct states of the dye that exhibit different rotational flexibility and different fluorescence lifetimes.38 Especially for cyanine dyes such as Cy3 and Cy5, it is well known that steric hindrance affects the isomerization rate to the non-fluorescent *cis* isomer, leading to an increase in

brightness and fluorescence lifetime.37,39,40 At early time lags, the anisotropy decay is dominated by the contribution of the short lifetime species while, at long time lags, only the long lifetime species contribute. After the initial decay of the anisotropy due to the fluorophore rotation, the decay levels off to a residual value r_∞ reporting on the slow rotation of the origami. The model to describe the decay (solid lines in Figure 4 A) is outlined in detail in the SI 8. In the singly-labeled constructs, the decay in anisotropy is due to rotation of the fluorophores. For the full construct, a larger drop in anisotropy is observed due to homo-FRET.41–44 Here, we focus only on the residual anisotropy r_∞ as an indicator of homo-FRET (Table 2).

The triple-labeled construct, $G_1G_2G_3$, showed the largest change in the residual anisotropy (Δr_∞= 0.052), a clear indication for efficient homo-FRET. All double-labeled constructs also exhibited a reduced residual anisotropy compared to the single-labeled constructs. The highest difference is observed for the construct XG_2G_3 (Δr_∞= 0.032), the lowest for G_1G_2X (Δr_∞= 0.014). Surprisingly, G_1XG_3 (Δr_∞=0.023) shows a higher change in residual anisotropy, and thus a higher efficiency of homo-FRET, than G_1G_2X, even though the distance between the dyes is larger (5.4 nm vs. 4.6 nm). The influence of the dipole-dipole orientation is an important factor in FRET.45 The measured anisotropies for the single-labeled constructs of $r_\infty \approx 0.22$ for donor and acceptor in the case of homo-FRET indicate a possible effect of the orientation on the transfer efficiency. Furthermore, the interdependence of the quantum yield and steric hindrance for Cy3 introduces a correlation between the rotational flexibility and the Förster radius. Thus, differences in the local environment or unfavourable orientation of the dipoles of the dyes could explain the higher efficiencies of homo-FRET for construct G_1XG_3 with respect to G_1G_2X. As a control, we measured a construct with large separation between the three Cy3 dyes, yielding no significant change in the residual anisotropy (r_∞=0.226) (Figure S4 for measurements and details on dyes arrangement).

We additionally investigated the fluorescence lifetime of the different constructs. In all cases, Cy3 showed a complex fluorescence decay, which we analyzed using a three-component exponential model function, as has been employed in previous studies of Cy3 covalently attached to DNA or proteins.38,40 The three lifetime components of the single-labeled constructs are 0.33 ± 0.08 *ns*, 1.14 ± 0.20 *ns* and *2*.60 ± 0.01 *ns*. In the following, we focus our discussion on the average fluorescence lifetime (see Table 2). Among the single-labeled constructs, G_2 shows a shorter average lifetime. We attribute the difference in lifetimes to the position on the origami structure and to the different way the fluorophore is linked to the staple strand. It is well known that the behavior of dyes, in particular their quantum yield and rotational flexibility, is influenced both by neighboring DNA bases through stacking interactions and sequence dependent enhancement and quenching and by the covalent coupling of the dye to DNA.37,40,46,47 The Cy3 molecule in position G_2 is the only one directly linked to a thymine base on a modified DNA strand, while the fluorophores in position G_1 and G_3 are terminally linked to the 5’ end of the DNA strands and an extra unpaired thymine base has been added as a spacer to prevent quenching from other DNA bases on the origami surface. Therefore, we attribute the difference in lifetime to the different linker flexibility and local environment surrounding the dyes. Furthermore the longer lifetime of positions G_1 and G_3 is likely caused by transient base-stacking

interactions with the unpaired thymine.37,40 Interestingly, looking at the average lifetime per molecule measured in our single-molecule experiments (Figure S5), we observe broad distributions ranging from at 0.6 ns to 2 ns. This observation indicates that the dye-origami interactions persist for timescales longer than the diffusion of origami through the observation volume of ~10 ms.

In general, all constructs with multiple green dyes show reduced lifetimes compared to the single-labeled ones. Theoretically, homo-FRET should not result in a change of the observed fluorescence lifetimes and the quantum yield.42 However, this conclusion only holds true when the dyes behave identically. The observed change of the fluorescence lifetime is larger for the triple-labeled construct, which also exhibits the highest decrease in anisotropy. We speculate that the decrease in lifetime is most likely a consequence of the existence of multiple lifetime components and homo-FRET leads to a higher population of the energy sinks. While the absolute values of the three lifetime components do not change by a large amount, the reduction of the average fluorescence lifetime is mostly caused by a decrease in the fraction of the long lifetime component (see SI 9: Table S5 and lifetime distribution plots Figure S5 and Figure S6). Due to the longer lifetime, this component is expected to be the major contributor to homo-FRET, resulting in a reduced contribution of this state to the total fluorescence decay. We speculate that the short lifetime state effectively serves as an energy sink during the homo-FRET process.

We have demonstrated that our intermediate dyes can perform homo-FRET and that this phenomenon does lead to higher energy transfer over the 10.5 nm distance of the dye assembly with respect to the single FRET pairs. However, any one of the three green dyes can be initially excited in the system. To localize the excitation and study directed energy transfer through the homo-FRET system, we investigated the full three-color cascade PW, where a blue primary donor is placed 5.4 nm from G_1 (cf. Figure 1). After verifying that no energy transfer occurs between the blue donor and the red acceptor without intermediate green dyes (SI 10 Figure S8), we separately measured the previous constructs in the presence of the blue fluorophore. To estimate the energy transfer efficiency from the blue donor to the red acceptor dye, we use the percentage of red signal after excitation of the blue dye. This apparent energy transfer efficiency for SM FRET is not corrected for spectral crosstalk or cross-excitation, and only serves as an indicator to compare the relative efficiency of the different constructs (see SI 11). The efficiency calculated for bulk measurements is corrected for spectral cross-talk, but not for cross-excitation (see SI 12). The presence of only one intermediate green dye results in very low or undetectable emission from the red acceptor ranging from 0.6 % to 1.3 % in bulk measurements and between 3 % to 5 % in SM measurements (Figure S9 and Table S7 for smFRET experiments and Figure SI10 and Table S9 for bulk experiments). Using the fluorescence lifetime of Alexa488 we estimate the FRET efficiency from the blue dye to the individual Cy3 positions to be 52 % to position G_3, 13 % to position G_2 and 4 % to position G_1 (see Table S8). For constructs with two green dyes, we observed an increase in the apparent transfer efficiency from the blue dye to the red fluorophore ranging from 5 % to 9 % for SM FRET and from 1.3 % to 3.3 % for bulk measurements. Our full photonic wire with all three Cy3s produces an increase in energy transfer efficiency to 5% measured in bulk (see SI 12 and Table S9 for efficiency estimation) and 10 % in the SM measurements (Table S7). To visualize this

Europe PMC Funders Author Manuscripts

increase, we compared the sum of the red emissions of all single Cy3 dye wires, $BXXG_3R$, BXG_2XR and BG_1XXR, with the complete wire $BG_1G_2G_3R$ (Figure 5). Since exciting the blue donor at 490 nm results in partial excitation of Cy3, we performed bulk measurements also with 460 nm excitation (see Figure S11). The results are fully consistent with the spectra obtained with excitation at 490 nm.

Finally, we modelled the three-color energy transfer process with MC simulations. When taking into account the partial direct excitation of Cy3 dyes, the calculated values are in very good agreement with our experimental findings (see Table S10). Most importantly, the overall transfer efficiency is 4.4%, which is significantly higher than the arithmetic sum of the constructs with only one intermediated green dye (2%).

Conclusion

In this work, we demonstrated a photonic wire mediated by a homo-FRET chain of three Cy3 fluorophores. Our observations show that homo-FRET amongst the Cy3 dyes can have an enhancing effect on the overall energy transfer to the acceptor fluorophore. The occurrence of homo-FRET between all Cy3 dyes was confirmed by a decrease of the fluorescence anisotropy. Furthermore, we found that homo-FRET can significantly change the fluorescence lifetime and thus quantum yield of Cy3, an effect that is not predicted from FRET theory alone. Lastly, we showed that energy can be transferred through the homo-FRET system from a blue donor dye to a red acceptor dye over a distance of 16 nm.

In summary, the energy transfer enhancement and the insights about the homo-FRET process investigated in our work can be utilized as a guide to extract design principles for complex light harvesting assemblies on biological platforms, such as DNA, protein capsids and lipid membrane as well as on artificial systems such as dye-sensitized solar cells.

Material and methods

Dyes and DNA origami

The DNA origami structure used in our experiments is a square lattice 3-layer brick-like structure (for origami design, DNA sequences and folding conditions see SI 14). The dyes were incorporated in the DNA structure during folding by adding the desired dye-labeled DNA strands in the mixture of ssDNA scaffold, staples and buffer. All the samples were purified with PEG precipitation 48,49 before performing fluorescence measurements.

The dye functionalized DNA strands were purchased from IBA GmbH, Göttingen, Germany. Both internal (on thymine base) and terminal (on 5’-end) functionalization were carried out through NHS ester coupling. For details on dye-labeled DNA strands see Table S11.

Bulk fluorescence spectroscopy

Bulk fluorescence measurements were carried out with a modular spectrofluorometer Fluorolog®3, Horiba scientific. For the measurements the sample was transferred into a cuvette 2x10mm optical path (Hellma Analytics). The samples consist of 100 uL of 10 nM

DNA origami carrying different dyes combinations in a buffer solution (10 mM Tris, 1 mM EDTA and 20 mM $MgCl_2$).

Each construct was independently assembled and measured at least six times. Fluorescence emission spectra were recorded and the FRET efficiency calculated from the relative intensities of the donor and acceptor fluorescence. To avoid direct excitation of Cy5, Cy3 was excited at 520 nm instead of its absorbance maximum at 555 nm. We normalized the emission spectra with respect to the Cy5 emission after excitation at 640 nm in order to correct for different sample concentrations.

Single molecule fluorescence

Single-molecule measurements of FRET efficiency, fluorescence lifetime and anisotropy were performed on a custom-build confocal microscope. DNA origami samples were diluted to concentrations of 100 pM in 10 mM Tris, 1 mM EDTA and 20 mM $MgCl_2$ and 1 mM Trolox to reduce photo blinking and bleaching. The fluorophores were excited using pulsed interleaved excitation (PIE)32 at the laser excitation lines 482 nm, 561 nm and 641 nm (LDH-D-C-485, LDH-D-TA-560, LDH-D-C-640, Picoquant, Berlin, Germany). Laser powers of 110 μW for the blue laser, 80 μW for the green laser, and 40 μW for the red laser, as measured before the objective, were used. Fluorescence was collected by a 60x water immersion objective (60x/1.27 WI, Nikon, Düsseldorf, Germany), separated from the excitation light by a polychroic mirror (zt405/488/561/633), and focussed through a 50 μm pinhole. It was then split according to polarization (PBS251, Thorlabs, Dachau, Germany), and wavelength (dichroic mirrors BS560 and 640DCXR) and filtered by the emission filters for blue (ET525/50), green (ET607/36), and red (ET670/30) fluorescence (AHF Analysentechnik, Tübingen, Germany). The signals were detected on six avalanche photodiodes (Count-100B, Laser Components, Olching, Germany; SPCM-AQR-14, SPCM-AQRH-14, Perkin Elmer, Hamburg, Germany) and recorded by time-correlated single-photon electronics (HydraHarp 400, Picoquant, Berlin, Germany). Data analysis was performed using custom software written in MATLAB.

Monte Carlo simulation on energy transfer efficiency

The emission from each dye was calculated by using Monte Carlo simulation that samples different orientation of fluorophores. The angle of fluorophore dipole θ and ϕ were isotropically varied from $-\pi$ to $-\pi$ and $-\pi/2$ to $-\pi/2$ respectively to take account of fluorophores rotating on the surface of a DNA nanostructure. The transfer rate from each Cy3 to Cy5 was calculated from the control bulk measurement while homo-transfer rate and Alexa 488 to Cy3 transfer rate was calculated from the spectral overlap *J*. We assume that a fluorophore in an excited state has 3 pathways – radiative decay, non-radiative decay and energy transfer. Radiative decay and non-radiative decay was calculated from the quantum yield of fluorophores. The orientation factor κ^2 was calculated from $\kappa = \hat{\mu}_D \cdot \hat{\mu}_A - 3(\hat{\mu}_D \cdot \hat{R}_{AD})(\hat{\mu}_A \cdot \hat{R}_{DA})$ where $\hat{\mu}_D$ and $\hat{\mu}_A$ are the normalized dipole moment of each fluorophores which undergo rotation while $\hat{R}_{AD}$ and $\hat{R}_{DA}$ denote normalized inter-fluorophore distance vector. We sampled 4000 configurations of angles over 10 transfer cycles which were enough to acquire converged emission from each fluorophore.

Supplementary Material

Refer to Web version on PubMed Central for supplementary material.

Acknowledgements

The authors are grateful for financial support from the European Commission through the ERC grant agreement n° 336440, ORCA, from the Deutsche Forschungsgemeinschaft (DFG) through the SFB1032 (Project A6 and B3) and the Ludwig-Maximillians-Universität München via the Center for NanoScience Munich (CeNS) and LMUinnovativ initiative BioImaging Network (BIN).

References

1. Scholes GD, Fleming GR, Olaya-Castro A, van Grondelle R. Lessons from nature about solar light harvesting. Nat Chem. 2011; 3:763–774. [PubMed: 21941248]
2. Hu X, Damjanović a, Ritz T, Schulten K. Architecture and mechanism of the light-harvesting apparatus of purple bacteria. Proc Natl Acad Sci U S A. 1998; 95:5935–5941. [PubMed: 9600895]
3. Van Amerongen H, Croce R. Light harvesting in photosystem II. Photosynth Res. 2013; 116:251–263. [PubMed: 23595278]
4. Cheng Y-C, Fleming GR. Dynamics of light harvesting in photosynthesis. Annu Rev Phys Chem. 2009; 60:241–62. [PubMed: 18999996]
5. Weckwerth W. Long-Range Resonance Energy Transfer in Molecular Systems. Annu Rev Plant Biol. 2003; 54:669–689. [PubMed: 14503007]
6. Andrews DL, Crisp RG. Theory of directed electronic energy transfer. J Fluoresc. 2006; 16:191–9. [PubMed: 16575550]
7. Daniels GJ, Jenkins RD, Bradshaw DS, Andrews DL. Resonance energy transfer: The unified theory revisited. J Chem Phys. 2003; 119:2264–2274.
8. Sumino A, et al. Selective assembly of photosynthetic antenna proteins into a domain-structured lipid bilayer for the construction of artificial photosynthetic antenna systems: Structural analysis of the assembly using surface plasmon resonance and atomic force microscopy. Langmuir. 2011; 27:1092–1099. [PubMed: 21204531]
9. Nagata N, Kuramochi Y, Kobuke Y. Energy transfer among light-harvesting macrorings incorporated into a bilayer membrane. J Am Chem Soc. 2009; 131:10–11. [PubMed: 19086896]
10. Nagata M, et al. Construction and photocurrent of light-harvesting polypeptides/zinc bacteriochlorophyll a complex in lipid bilayers. Chem Lett. 2003; 32:852–853.
11. Bhosale S. Photoproduction of Proton Gradients with -Stacked Fluorophore Scaffolds in Lipid Bilayers. Science (80-.). 2006; 313:84–86.
12. Nam YS, et al. Virus-templated assembly of porphyrins into light-harvesting nanoantennae. J Am Chem Soc. 2010; 132:1462–1463. [PubMed: 20078048]
13. Park H, et al. Enhanced energy transport in genetically engineered excitonic networks. Nat Mater. 2015; 15:211–216. [PubMed: 26461447]
14. Mishra A, Fischer MKR, Bäuerle P. Metal-Free organic dyes for dye-Sensitized solar cells: From structure: Property relationships to design rules. Angew Chemie - Int Ed. 2009; 48:2474–2499.
15. Buckhout-White S, et al. Assembling programmable FRET-based photonic networks using designer DNA scaffolds. Nat Commun. 2014; 5
16. Dutta PK, et al. DNA-directed artificial light-harvesting antenna. J Am Chem Soc. 2011; 133:11985–11993. [PubMed: 21714548]
17. Hemmig EA, et al. Programming Light-Harvesting Efficiency Using DNA Origami. Nano Lett. 2016; 16:2369–2374. [PubMed: 26906456]
18. Melinger JS, et al. FRET from Multiple Pathways in Fluorophore-Labeled DNA. ACS Photonics. 2016; 3:659–669.
19. Hannestad JK, Gerrard SR, Brown T, Albinsson B. Self-assembled DNA-based fluorescence waveguide with selectable output. Small. 2011; 7:3178–3185. [PubMed: 21901828]

20. Adeyemi OO, Malinovskii VL, Biner SM, Calzaferri G, Häner R. Photon harvesting by excimer-forming multichromophores. Chem Commun. 2012; 48:9589.
21. Albinsson B, Hannestad JK, Börjesson K. Functionalized DNA nanostructures for light harvesting and charge separation. Coord Chem Rev. 2012; 256:2399–2413.
22. Díaz SA, et al. Extending DNA-Based Molecular Photonic Wires with Homogeneous Förster Resonance Energy Transfer. Adv Opt Mater. 2016; 4:399–412.
23. Hannestad JK, Sandin P, Albinsson B. Self-assembled DNA photonic wire for long-range energy transfer. J Am Chem Soc. 2008; 130:15889–15895. [PubMed: 18975869]
24. Graugnard E, et al. DNA-controlled excitonic switches. Nano Lett. 2012; 12:2117–2122. [PubMed: 22401838]
25. Cannon BL, et al. Excitonic and logic gates on DNA brick nanobreadboards. ACS Photonics. 2015; 2:398–404. [PubMed: 25839049]
26. Tinnefeld P, Heilemann M, Sauer M. Design of molecular photonic wires based on multistep electronic excitation transfer. ChemPhysChem. 2005; 6:217–222. [PubMed: 15751339]
27. Stein IH, Schüller V, Böhm P, Tinnefeld P, Liedl T. Single-molecule FRET ruler based on rigid DNA origami blocks. ChemPhysChem. 2011; 12:689–695. [PubMed: 21308944]
28. Stein IH, Steinhauer C, Tinnefeld P. Single-molecule four-color FRET visualizes energy-transfer paths on DNA origami. J Am Chem Soc. 2011; 133:4193–4195. [PubMed: 21250689]
29. Zhang T, et al. DNA-Based Self-Assembly of Fluorescent Nanodiamonds. J Am Chem Soc. 2015; 137:9776–9779. [PubMed: 26196373]
30. Schreiber R, et al. Hierarchical assembly of metal nanoparticles, quantum dots and organic dyes using DNA origami scaffolds. Nat Nanotechnol. 2013; 9:74–78. [PubMed: 24292513]
31. Fischer S, et al. Shape and interhelical spacing of DNA origami nanostructures studied by small-angle X-ray scattering. Nano Lett. 2016; 16:4282–4287. [PubMed: 27184452]
32. Kudryavtsev V, et al. Combining MFD and PIE for Accurate Single-Pair Förster Resonance Energy Transfer Measurements. ChemPhysChem. 2012; 13:1060–1078. [PubMed: 22383292]
33. Cunningham PD, et al. Resonance Energy Transfer in DNA Duplexes Labeled with Localized Dyes. J Phys Chem B. 2014; 118:14555–14565. [PubMed: 25397906]
34. Di Fiori N, Meller A. The Effect of dye-dye interactions on the spatial resolution of single-molecule FRET measurements in nucleic acids. Biophys J. 2010; 98:2265–2272. [PubMed: 20483335]
35. Nicoli F, et al. Proximity-Induced H-Aggregation of Cyanine Dyes on DNA-Duplexes. J Phys Chem A. 2016; 120:9941–9947. [PubMed: 27934475]
36. Iqbal A, et al. Orientation dependence in fluorescent energy transfer between Cy3 and Cy5 terminally attached to double-stranded nucleic acids. Proc Natl Acad Sci U S A. 2008; 105:11176–81. [PubMed: 18676615]
37. Spiriti J, Binder JK, Levitus M, Van Der Vaart A. Cy3-DNA stacking interactions strongly depend on the identity of the terminal basepair. Biophys J. 2011; 100:1049–1057. [PubMed: 21320450]
38. Stennett EMS, Ciuba MA, Lin S, Levitus M. Demystifying PIFE: The Photophysics behind the Protein-Induced Fluorescence Enhancement Phenomenon in Cy3. J Phys Chem Lett. 2015; 6:1819–1823. [PubMed: 26263254]
39. Stennett EMS, Ma N, Van Der Vaart A, Levitus M. Photophysical and dynamical properties of doubly linked Cy3-DNA constructs. J Phys Chem B. 2014; 118:152–163. [PubMed: 24328104]
40. Sanborn ME, Connolly BK, Gurunathan K, Levitus M. Fluorescence properties and photophysics of the sulfoindocyanine Cy3 linked covalently to DNA. J Phys Chem B. 2007; 111:11064–11074. [PubMed: 17718469]
41. Berberan-Santos MN, Valeur B. Fluorescence depolarization by electronic energy transfer in donor–acceptor pairs of like and unlike chromophores. J Chem Phys. 1991; 95:8048.
42. Runnels LW, Scarlata SF. Theory and application of fluorescence homotransfer to melittin oligomerization. Biophys J. 1995; 69:1569–1583. [PubMed: 8534828]
43. Lidke DS, et al. Imaging molecular interactions in cells by dynamic and static fluorescence anisotropy (rFLIM and emFRET). Biochem Soc Trans. 2003; 31:1020–1027. [PubMed: 14505472]

44. Weber G. Dependence of the polarization of the fluorescence on the concentration. Trans Faraday Soc. 1954; 50:552.
45. Ivanov V, Li M, Mizuuchi K. Impact of emission anisotropy on fluorescence spectroscopy and FRET distance measurements. Biophys J. 2009; 97:922–929. [PubMed: 19651051]
46. Harvey BJ, Levitus M. Nucleobase-specific enhancement of Cy3 fluorescence. J Fluoresc. 2009; 19:443–448. [PubMed: 18972191]
47. Kretschy N, Sack M, Somoza MM. Sequence-Dependent Fluorescence of Cy3- and Cy5-Labeled Double-Stranded DNA. Bioconjug Chem. 2016; 27:840–848. [PubMed: 26895222]
48. Stahl E, Martin TG, Praetorius F, Dietz H. Facile and Scalable Preparation of Pure and Dense DNA Origami Solutions. Angew Chemie Int Ed. 2014; 53:12735–12740.
49. Douglas SM, Chou JJ, Shih WM. DNA-nanotube-induced alignment of membrane proteins for NMR structure determination. Proc Natl Acad Sci. 2007; 104:6644–6648. [PubMed: 17404217]

Europe PMC Funders Author Manuscripts

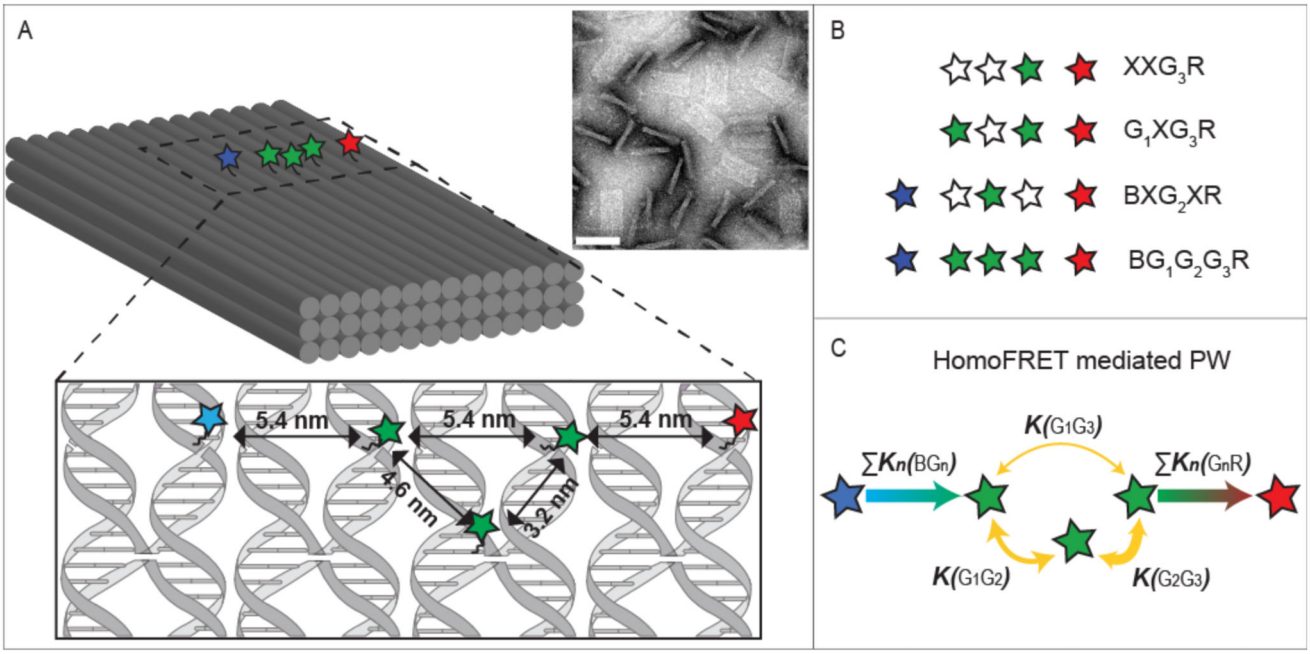

Figure 1. Homo-FRET-mediated photonic wire.

(A) Schematic representation of the three-layered DNA origami block and a TEM image of origami blocks, some of which are lying flat and others standing on their sides (scale bar: 80 nm). In the enlarged region, the scheme indicates the designed locations of the dye molecules with respect to the DNA strands. (B) Examples of wire constructs introducing the nomenclature. Alexa488, Cy3 and Cy5 dyes are depicted as blue, green and red stars, respectively. Empty stars indicate the absence of a dye at this position. (C) Possible energy pathways of the photonic wire and their corresponding transfer rates. The thickness of the yellow arrows is proportional to the calculated efficiency of the homo-FRET between the two green dyes.

Europe PMC Funders Author Manuscripts

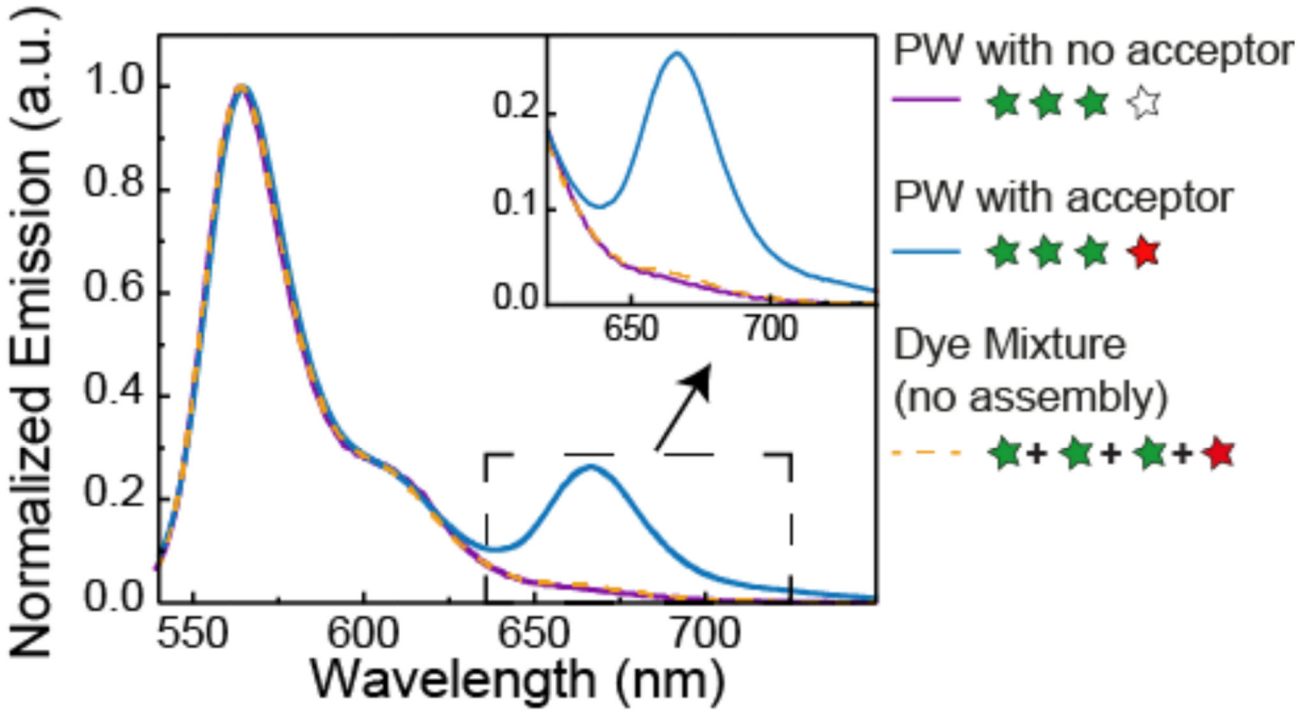

Figure 2. FRET vs. non-FRET emission spectra.

Bulk emission spectra of the homo-FRET photonic wire with (blue line) and without (purple line) acceptor dye and the mixture of Cy3/Cy5 labeled DNA staples which constitute the photonic wire (orange dashed line), upon 520 nm incident light.

Europe PMC Funders Author Manuscripts

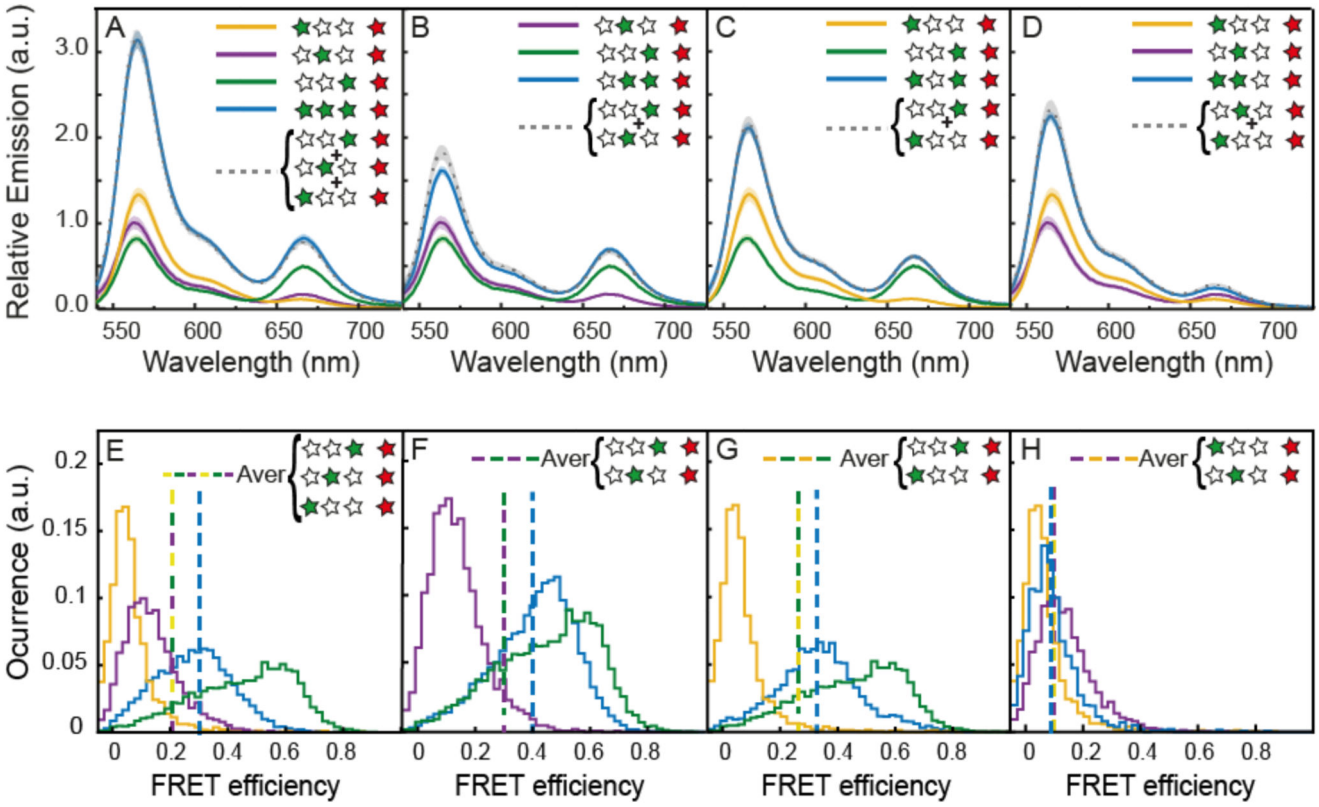

Figure 3. Two-color cascade.

(Top panel A-D) bulk emission spectra of constructs carrying a variable number of Cy3 dyes and a single Cy5 acceptor. The recorded emission intensities are normalized by the intensity of the Cy5 emission after Cy5 excitation in order to account for differences in sample concentration. The shading around the plotted lines indicate the error of the mean (the final spectra are the result of an average of multiple measurements on at least 6 different sample batches). The comparison between the spectra of the constructs containing two Cy3 dyes (blue lines) and the mathematical sum of the spectra of the respective partial constructs with only one Cy3 (gray lines) is shown for XG_2G_3R (A), G_1XG_3R (B), G_1G_2XR (C) and $G_1G_2G_3R$ (D). (Bottom panel E-H) SM FRET histograms of constructs carrying a variable number of Cy3 dyes and a single Cy5 acceptor. Occurrence values are normalized by the histogram areas. Each histogram contains at least 2000 events. Dashed lines indicate the average efficiency.

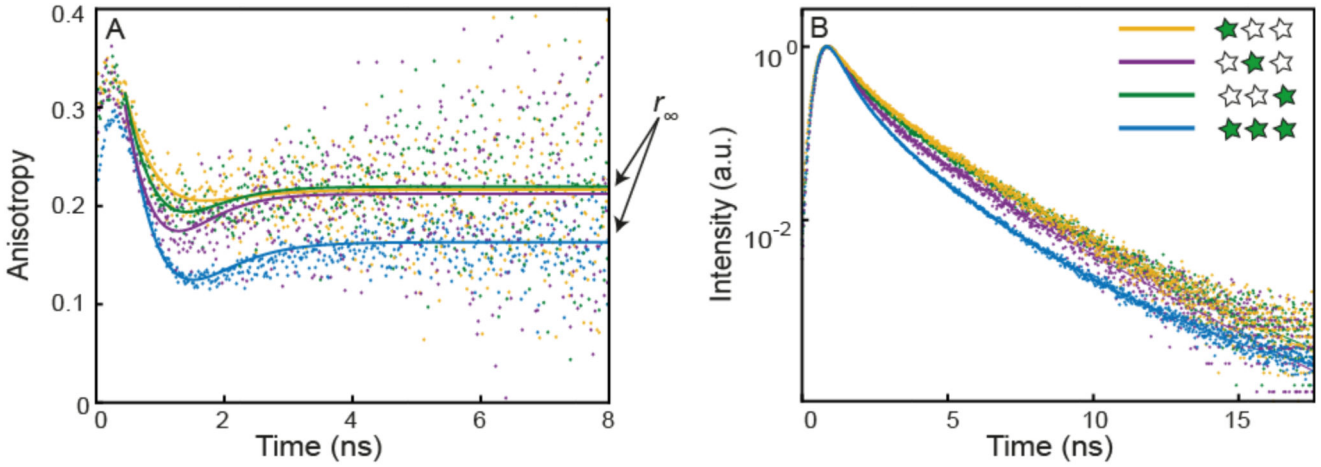

Figure 4. Single-molecule fluorescence anisotropy and fluorescence lifetimes

(A) Time-resolved fluorescence anisotropy decays of Cy3-labeled DNA origami. The anisotropy decays of the single labeled constructs, G_1, G_2 and G_3 (orange, purple and green line, respectively) show similar behavior while the decay of the triple-labeled construct ($G_1G_2G_3$, blue line) shows decreased anisotropy confirming homo-FRET occurrence. (B) Fluorescence lifetimes of the same constructs. The lifetime decay of $G_1G_2G_3R$ (blue) shows a reduction in lifetime compared to that of the single-labeled constructs.

Europe PMC Funders Author Manuscripts

Europe PMC Funders Author Manuscripts

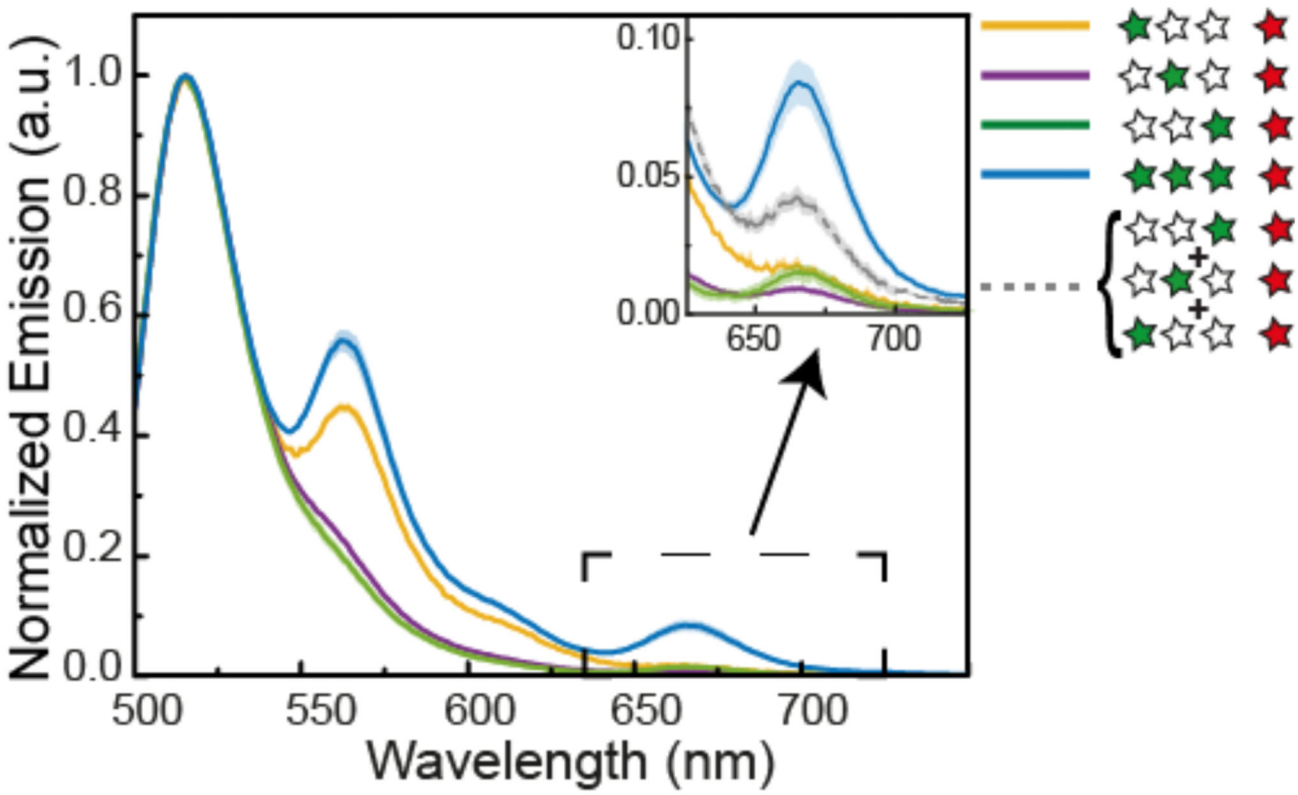

Figure 5. Three-color cascade.

(A) Normalized emission spectra of the three-color cascade after Alexa488 excitation. Due to spectral overlap between Alexa488 and Cy3, the green emission peak around 550 nm becomes only apparent for constructs where the closest dye to the blue donor is present. Inset: Zoom into the Cy5 emission spectral region. Wires with only one green dye do not show a significant emission of the red acceptor. Cy5 emission appears when all three Cy3 dyes are present. The gray line represents the arithmetic sum of the red signals from BG_1XXR, BXG_2XR and $BXXG_3R$, which is significantly lower than the red emission from $BG_1G_2G_3R$.

Europe PMC Funders Author Manuscripts

Table 1

FRET efficiencies with their absolute error from bulk and SM measurements as well as MC calculations. The efficiency increment ΔE is calculated as the difference between the averaged efficiency of single hetero-FRET pairs and their corresponding homo-FRET construct.

	G_1XXR	XG_2XR	XXG_3R	G_1G_2XR	G_1XG_3R	XG_2G_3R	$G_1G_2G_3R$
E_{Bulk}	0.05 ±0.004	0.12 ±0.009	0.36 ±0.02	0.07 ±0.004	0.21 ±0.009	0.29 ±0.01	0.19 ±0.001
ΔE				-0.015 ±0.011	0.000 ±0.025	0.040 ±0.027	0.011 ±0.028
E_{SM}	0.06 ±0.002	0.13 ±0.002	0.45 ±0.002	0.09 ±0.002	0.33 ±0.002	0.4 ±0.001	0.28 ±0.002
ΔE				-0.01 ±0.003	0.07 ±0.003	0.11 ±0.003	0.06 ±0.004
E_{MC}	0.03	0.10	0.28	0.07	0.15	0.22	0.15
ΔE				0.005	-0.005	0.025	0.014

Europe PMC Funders Author Manuscripts

Table 2

Residual fluorescence anisotropy (r_∞) and average fluorescence lifetime (τ) of single- and triple-labeled Cy3 constructs. Δr_∞ and $\Delta\tau$ indicate the differences of these values for the multi-dye constructs with respect to the average value of the single-dye constructs. Errors are given as 95% confidence intervals.

	G_1XX	XG_2X	XXG_3	$G_1G_2G_3$	G_1G_2X	G_1XG_3	XG_2G_3
r_∞	0.219 ±0.007	0.216 ±0.009	0.223 ±0.006	0.167 ±0.004	0.203 ±0.007	0.198 ±0.004	0.188 ±0.006
Δr_∞				*0.052* ±0.006	*0.014* ±0.009	*0.023* ±0.006	*0.032* ±0.008
τ (ns)	1.57 ±0.04	1.34 ±0.06	1.52 ±0.09	1.09 ±0.03	1.20 ±0.07	1.27 ±0.02	1.27 ±0.05
$\Delta\tau$ (ns)				*0.40* ±0.05	*0.27* ±0.08	*0.27* ±0.05	*0.16* ±0.07